

MAGNETIC STUDIES OF ACTINIDES--EVIDENCE FOR LOCALIZED MAGNETISM

By



G. H. Lander

NOTICE

This report was prepared as an account of work performed by the United States Government. Neither the United States nor the United States Energy Research and Development Administration, nor any of their employees, nor any of their contractors, subcontractors, or their employees, makes any warranty, express or implied, or assumes any legal liability or responsibility for the accuracy, completeness, or usefulness of any information, apparatus, product, or process disclosed, or represents that its use would not infringe privately owned rights.

Prepared For Presentation at
21st Annual Conference on
Magnetism and Magnetic Materials
Philadelphia, PA.
December 9-12, 1975



U of C AUS-USERDA

ARGONNE NATIONAL LABORATORY, ARGONNE, ILLINOIS

operated under contract W-31-109-Eng-38 for the
U. S. ENERGY RESEARCH AND DEVELOPMENT ADMINISTRATION

MAGNETIC STUDIES OF ACTINIDES--EVIDENCE FOR LOCALIZED
MAGNETISM*

G. H. Lander
Argonne National Laboratory, Argonne, Ill. 60439

ABSTRACT

The position of the $5f$ elements in the periodic table suggests that the electronic properties of these elements (and their compounds) will resemble those of the lanthanide series. However, the extended nature of the $5f$ wave functions leads to fundamental differences between $4f$ and $5f$ systems. In this review the evidence for "localized" magnetism will be presented. Results of magnetization, Mössbauer, neutron and low-temperature x-ray experiments on Np, Pu, and Am compounds will be used to illustrate both the similarities to and differences from lanthanide magnetism.

A determination of the ground-state $5f$ electron wave functions is, in principle, possible by measuring the neutron magnetic cross section. The interpretation of such experiments on UO_2 , USb, and PuP requires a knowledge of the radial extent of the $5f$ electrons, which we obtain from relativistic Dirac-Fock calculations, and the use of the tensor-operator formalism to treat the spin-orbit interaction. This interaction in Pu^{3+} (a $5f^5$ configuration) results in a magnetic form factor that initially increases with increasing scattering angle. For USb the experimental magnetic scattering is used to determine the ground-state wave function of the U^{3+} ion. In addition the temperature dependence of the quadrupole moment in USb has been measured and yields information both on the size of the crystal-field and exchange interactions, and on the interplay between them.

INTRODUCTION

The unique problems associated with describing the electronic structure of the actinide elements and compounds were recognized as soon as the first investigations were performed some 35 years ago. A consequence of the spatial extent of the outermost electrons is that the actinide ions are sensitive to their environment, i.e., large crystal-field interactions are present.¹ On the other hand, the $5f$ electrons have a high angular momentum state, and the term $l(l+1)/r^2$ in the Schrödinger equation then acts in combination with the atomic potential to produce a centrifugal barrier confining the electron to an annular region around the nucleus, i.e., the spin-orbit coupling is large.² The presence of both large spin-orbit and crystal-

field interactions leads to complications that are rarely found in either the 3d transition series, in which the crystal field dominates, or the lanthanide (4f) series, in which the spin-orbit term dominates.

What are those properties of the system that suggest the presence of localized 5f electrons? (1) A large spin-orbit coupling, i.e., the tendency for the spin and angular momenta to combine together in such a way as to produce a good quantum number J . Of course, the presence of a large crystal-field interaction may break down Russell-Saunders coupling, necessitating the use of intermediate-coupling g factors and even J mixing.² (2) The high-temperature susceptibility should reflect the localized moment behavior giving an effective moment $\mu_{\text{eff}} = g \sqrt{J(J+1)}$. (3) If conduction electrons are present to mediate the signal between nonmagnetic and actinide ions the nuclear spin-lattice relaxation rate $1/T_1$ at the anion will sense the induced moment (i.e., the susceptibility) at the actinide site. (4) As a consequence of the large orbital moment (excluding S-state ions) (a) an appreciable spin-lattice interaction should exist. In turn, this leads to magnetic anisotropy and the probable crystallographic distortion of the chemical unit cell in order to minimize the magnetoelastic energy. (b) A large orbital contribution to the hyperfine field will be present at the actinide nucleus. (5) The crystal-field interaction will lift the degeneracy of the J multiplets and result in wave functions that reflect the symmetry of the actinide ion. Such a representation implies the presence of well defined spin-wave excitations, which reflect both the crystal-field and exchange interactions in the material.

By attempting to characterize the 5f electrons as localized we are, of course, assuming that the 5f bands have a narrow energy distribution in momentum space and that their energies lie well below the Fermi energy E_F . Extensive band-structure calculations have been performed on the actinide elements,¹ all showing that the 5f states are neither narrow nor well below E_F . Davis has presented a preliminary calculation for the NaCl compounds.³ The presence of f electrons near E_F contributes to the peak in the density of states. Such a peak is compatible with the high values for the electronic specific heat, which, in mJ/mole K^2 , are 23.3, 9.6, and 49.0 for US, UP, and UN, respectively. Although hybridization makes it difficult to define the 5f bandwidth, the average value suggested by the band calculations is 2 - 3 eV, as opposed to ~ 0.3 eV for the localized 4f electrons. uv photoemission spectra⁴ on US have been interpreted as supporting the itinerant picture of the 5f electrons in this compound, although Veal has argued for a more cautious approach in connecting theory and experiment.⁵ We will return to US later; the important point of introducing the band-

structure ideas is that we do not expect any one model to correctly describe all the properties of these actinide compounds.

In the elemental metals, at least for the first half of the series, the spatial extent and corresponding wave function overlap causes a situation which requires a description in terms of itinerant $5f$ electrons. The concept of spin fluctuations (i.e., incipient magnetic behavior) appears to explain the resistivity, specific heat, and susceptibility.⁶ Attempts to provide more direct evidence of such phenomena with microscopic techniques, such as nuclear-gamma-ray resonance or neutron scattering are difficult, but worthwhile, endeavors for future research.

In this article we will concentrate almost exclusively on the actinide compounds that form with elements of Group VA and VIA of the periodic table and crystallize in the NaCl structure. In the first part we will discuss magnetization, nuclear-gamma-ray resonance (Mössbauer), neutron and low-temperature x-ray experiments. In the second part we will present results from recent "second generation" neutron experiments on single crystals of uranium compounds.

ACTINIDE COMPOUNDS WITH THE NaCl CRYSTAL STRUCTURE

Some properties of actinide compounds with the NaCl structure⁷⁻⁹ are given in Table I. All these compounds are metallic with resistivities ranging between 100 and 2000 $\mu\Omega$ cm. The presence of conduction electrons and their possible interaction with the $5f$ electrons must therefore be kept in mind. The object in studying the trends in such a table is to see if unique $5f$ electron configurations can be assigned, as is the case for example, in similar lanthanide ($4f$) compounds. If the actinide ions are trispositive, the configurations will be $U^{3+} - f^3$, $Np^{3+} - f^4$, $Pu^{3+} - f^5$, and $Am^{3+} - f^6$. The actinide contraction will favor these configurations as one proceeds to the heavier ions and this is confirmed by the large effective moments of Cm and Bk ($\sim 8\mu_B$), which suggest f^7 and f^8 configurations, respectively.⁶ The spatial extent of the $5f$ wave functions means that those compounds with the smallest lattice spacings may have the most complicated behavior. Indeed Hill¹⁰ proposed a direct correlation between the $An - An$ separation and the occurrence of magnetic order, with the critical separation being about 3.4 Å, i.e., $a_0 \sim 5.1 \text{ \AA}$ in the NaCl structure.

Starting with the heavier ions in Table I, $AmSb$ exhibits temperature independent susceptibility. This behavior is consistent with, but does not necessarily prove, the existence of a $5f^6: ^7F_0$ ground state. The situation for PuS is similar. All the remaining Pu compounds exhibit low effective magnetic moments ($\sim 1 \mu_B$)

and ordered moments of between 0.4 and 0.8 μ_B . These values are consistent with a $5f^5:6H_{5/2}$ configuration. As we discuss in more detail below, the magnetic form factor of this configuration is sufficiently unique that measurements of the neutron magnetic cross section, even from polycrystalline samples, unambiguously defines the ground state. However, for f^5 states (both Sm and Pu) the excited J multiplet is fairly close in energy to the ground state. This means that the effects of intermediate coupling and J mixing may be appreciable.

Assignments for the neptunium and uranium compounds are not nearly as straightforward. For example, the effective magnetic moment μ_{eff} of f^2 , f^3 , and f^6 free-ion states are 3.58, 3.62 and 2.68 μ_B , respectively. The ordered moments μ_{sat} are 3.20, 3.27, and 2.40 μ_B , respectively. With the added complications of crystal-field and exchange effects the identification of the configuration from either μ_{eff} or μ_{sat} may be ambiguous. The Np compounds have ordered moments ranging between 1.4 and 2.5 μ_B , and the values of μ_{eff} are also consistent with a $5f^4$ configuration. For Np compounds additional information is available from Mössbauer-effects measurements. The hyperfine field H_{hf} consists of a core contribution, taken in the first approximation to be proportional to $\langle S_z \rangle = \chi(g_J - 1) \langle J_z \rangle$, and an orbital contribution proportional to $\langle J || N || J \rangle \langle r^{-3} \rangle \langle J_z \rangle$, where $\langle J || N || J \rangle$ is a reduced matrix element dependent on the ionic configuration, and $\langle r^{-3} \rangle$ is the average value of $1/r^3$ for the open-shell electrons. Thus, $H_{\text{hf}} \propto \langle J_z \rangle = \mu_{\text{sat}}/g_J$. In Fig. 1 we show the correlation¹¹ between the hyperfine field and the ordered moment as determined by neutron diffraction. Of particular interest is that the linear relationship, $H_{\text{hf}} = (1915 \pm 50) \mu_{\text{sat}} \text{ kOe}/\mu_B$, extrapolates through the Np^{3+} value (corresponding to a $5f^4$ configuration) calculated with intermediate-coupling wave functions and relativistic values for $\langle r^{-3} \rangle$. Another feature of the correlation is that it extends to values of μ_{sat} less than 1 μ_B , as found in the Laves phase compounds.¹² Such a result indicates that the value of $\langle r^{-3} \rangle$ for the $5f$ electrons remains constant in these neptunium compounds.

The uranium compounds in Table I have been examined with a variety of experimental techniques and have been discussed with both a localized f electron formalism,² and an itinerant band-structure approach.³ As stated above, we expect to need both models to understand all the magnetic properties. For the compounds UP, UAs, and USb, which all have reasonably large U - U spacings, the localized $5f^3$ configuration appears appropriate. The situation is more complicated for UC, UN, and US. With a f^3 configuration and the octahedral coordination of the NaCl structure the crystal-field interaction leads to a quartet Γ_8 , or a magnetic doublet Γ_6 as the ground state. Assuming the predominance of the fourth-order term $V_4 \approx$

$A_6 \langle r^6 \rangle$, in comparison to the sixth-order term V_6 , the ordered moments μ_{sat} should lie between 1.73 and 2.55 μ_B . The intermediate coupling g factor is 0.7595, as compared to the $^4I_{9/2}$ value of $8/11 = 0.7273$, and we do not expect J mixing to perturb μ_{sat} by more than $\pm 10\%$. However, UC is nonmagnetic and UN, although it has a large μ_{eff} of $3.1 \mu_B$, orders with a moment of only $0.75 \mu_B$. Alternatively, both materials may be considered $5f^2$ states, in which the ground state may be a nonmagnetic singlet. The magnetic ordering in such a system is then induced by an exchange field large enough to mix the ground and excited (magnetic) states. This model has achieved quantitative success in Pr, Tb, and Tm compounds.¹³ The crystal-field splitting $E(\Gamma_4) - E(\Gamma_1)$ necessary to produce the temperature-independent susceptibility in UC is ~ 1500 K (130 meV). This is too large an energy separation to be observed directly with present neutron spectrometers, and the determination of the ground state by fitting the magnetic susceptibility should be treated with caution (see below). In the case of UN attempts to measure the spin-wave spectra are currently in progress.

SPIN LATTICE INTERACTIONS

In the discussions above we have not shown explicitly how the determination of the easy axis of magnetization and the occurrence of lattice deformations relates to the localization of $5f$ electrons, except in the sense that these effects are a consequence of a strong spin-lattice interaction mediated by the orbital moment. With the exception of Ce compounds, both the easy axis and lattice distortions are understood in the lanthanide series in terms of the crystal-field ground states. Such descriptions present problems for actinide compounds. For example, in Table I we note that in both U and Np compounds the easy axis are $\langle 100 \rangle$ for antiferromagnets and $\langle 111 \rangle$ for ferromagnets. The correlations thus appear with the magnetic structures rather than with the ground-state configuration. The temperature dependence of the lattice parameters of NpP and NpAs (Fig. 2) present evidence for very dramatic and unusual spin-lattice interactions.⁹ For the commensurate long-range magnetic structures ($T \leq 74$ K in NpP with a $3+$, $3-$ layered structure, and $142 < T < 175$ K in NpAs with a $4+$, $4-$ structure) tetragonal distortions are observed. However, for magnetic ordering incommensurate⁸ with the lattice ($74 < T < 130$ K in NpP), or the simple type I $+$, $-$ structure in NpAs, the lattice is apparently cubic. The effect in NpAs, in which the symmetry is raised (from tetragonal to cubic) in the ordered state, is so unusual that one is tempted to suggest a valence change occurs at 142 K. The electrical resistivity changes by an order of magnitude at this transition.⁸ Notice, however, that distortions in all type I antiferromagnets are absent, or at

least very small,^{9,14} $(c-a)/a \leq 10^{-3}$. At present no explanation for these spin-lattice interactions has been advanced. Recently, neutron experiments at Argonne on antiferromagnetic UO_2 , have shown that an internal shear deformation of the oxygen sublattice occurs below T_N , whereas the uranium atoms do not move.¹⁵ The magneto-elastic energy is minimized by this internal strain, which dominates the magnetic behavior of UO_2 , through strong spin-lattice coupling,¹⁶ and the symmetry of the overall unit cell remains unchanged. Although UO_2 is an insulator and has the fluorite structure, the general formulation of this new effect may also apply to the NaCl compounds. Indeed, similar effects have been proposed for certain lanthanide compounds.¹⁷

ELECTRON WAVE FUNCTIONS DETERMINED BY NEUTRON SCATTERING

The scattering of thermal neutrons yields, in principle, information about the radial and angular distributions of the unpaired electrons in a solid. In practice, achieving this goal is difficult. The experiments require accurate measurements from single crystals, and comparison with theory requires the use of the tensor-operator method¹⁸ together with relativistic values for the one-electron radial integrals.¹⁹

The magnetic scattering length is defined as a vector \vec{E}_Q , with spherical components E_Q given by

$$(2\pi \hbar/m) E_Q = \langle \psi_e | T_Q^K (e, \kappa) | \psi_e \rangle \quad (1)$$

The electron wave functions are represented by ψ_e and $T_Q^K (e, \kappa)$ defines a tensor operator. The neutron-electron interaction is expressed as a tensor of rank one, so that we need to evaluate three terms, $Q = 0, \pm 1$. The presence of an unquenched orbital moment means that the magnetization density is a vector quantity^{20,21} with three components, M_x , M_y , and M_z . We may associate the components E_Q as follows, $E_0 \rightarrow M_z$, $E_{+1} \rightarrow -(M_x + i M_y)/\sqrt{2}$, and $E_{-1} \rightarrow (M_y - i M_x)/\sqrt{2}$. The magnetic moment density is therefore obtained by Fourier transforming M_x , M_y , and M_z . In certain cases M , the total magnetization, may be perpendicular to the scattering vector κ (this is common practice in experiments with polarized neutrons), and then $E_{+1} = E_{-1} = 0$, and the moment density is a scalar quantity as is found in most transition metal compounds. We may write $E_0 = -2 \mu q^2$, where $\mu = (0.27 \times 10^{-12}) \mu_B(\kappa) \text{ cm}$ is the conventional magnetic scattering length, μ is the magnetic moment in Bohr magnetons, q^2 is the square of the magnetic interaction vector, and $f(\kappa)$ is the form factor, which is related to the magnetization density through the Fourier transform

$$\mu f(\kappa) = \int M(\vec{r}) e^{i\kappa \cdot \vec{r}} dr. \quad (2)$$

In the tensor-operator formalism

$$f(\kappa) = \langle j_0 \rangle + c_2 \langle j_2 \rangle + c_4 \langle j_4 \rangle + c_6 \langle j_6 \rangle \quad (3)$$

where

$$\langle j_i \rangle = \int_0^\infty U^2(r) j_i(\kappa r) dr \quad (4)$$

are the radial integrals of the one-electron wave functions and $j_i(\kappa r)$ are spherical Bessel functions. The coefficients c_i are defined by the electronic configuration of the magnetic ion and the experimental conditions. From these equations, assuming we know the magnetic moment μ (obtained by extrapolating the cross section to $\kappa = 0$), and the geometric term q^2 , an effective magnetic form factor $f'(\kappa)$ can always be deduced from both the observed and calculated cross sections. If $q^2 = 1$ then $E_{+1} = E_{-1} = 0$ and $f' = f$ as in Eq. (2); but, in general, the situation is more complex.

Accurate form-factor measurements have been reported for UO_2 (both in the ordered and paramagnetic states) and US. For UO_2 in the ordered state the ambiguity in the magnetic moment direction requires that the coefficients c_i in Eq. (3) be averaged over the (001) plane before comparing with experiment; thus losing a great deal of information about the anisotropy of the ground state. In the paramagnetic state²² the induced moment of $0.0374 \mu_B$ is too small to be able to compare $f(\kappa)$ values calculated with different models. However, this experiment does show that the radial integrals $\langle j_i \rangle$ of Eq. (4) derived from relativistic Dirac-Fock calculations¹⁹ are a good representation of the spatial extent of the $5f$ electrons in UO_2 .

Polarized neutrons have been used to measure the magnetic form factor²³ in ferromagnetic US. The neutron data suggests a magnetic moment of $1.70 \mu_B$, whereas magnetization experiments²³ give only $1.55 \mu_B$. Similar discrepancies occur in 3d transition metals and compounds and are ascribed to conduction-electron polarization. In US, it probably arises from hybridization of the $5f$, 6d, and 7s bands and, because of spatial delocalization of these wave functions, contributes to $f(\kappa)$ only for $\sin\theta/\lambda < 0.1 \text{ \AA}^{-1}$. The form factor of the localized part is shown in Fig. 3. The data do not depart much from a smooth curve, and we would expect considerable more anisotropy for $5f^3$ and $5f^4$ states. We have reanalyzed this data with the relativistic $\langle j_i \rangle$ integrals and, in agreement with Wedgwood's original analysis, obtain the best fit (open points in Fig. 3) for the $5f^2:\Gamma_1$ singlet configuration.

Considerably more anisotropy is present in the magnetic form factor of USb, see Fig. 4. The overall fit with a $5f^3:\Gamma_8^{(1)}$ ground state is excellent, again showing

the accuracy of the $\langle j_i \rangle$ integrals. The anisotropy in Fig. 4 allows us to distinguish between a number of possible ground states. We define a term

$$\Delta f = f(\vec{k}_1) - f(\vec{k}_2) \quad (5)$$

where $|\vec{k}_1| = |\vec{k}_2|$. From Eq. (3) we see that this eliminates the (spherically symmetric) term in $\langle j_0 \rangle$ and focuses on higher-order integrals that reflect the magnetic quadrupole, octapole, and higher moments. In Fig. 5 Δf for a number of pairs of reflections is plotted versus $\sin\theta/\lambda$. Assuming the LLW parameter $x = 0.8$, (x reflects the ratio between V_4 and V_6 , and the analyses are independent of x for $0.7 < x < 1.0$. The sign of x depends on the coordination only) the ground-state wave functions are

$$W<0 \quad \Gamma_8^{(2)} \quad \psi_e = 0.79|9/2\rangle - 0.59|1/2\rangle - 0.14|-7/2\rangle,$$

$$\mu_{\text{sat}} = 2.12 \mu_B$$

$$W>0 \quad \Gamma_8^{(1)} \quad \psi_e = 0.97|7/2\rangle - 0.25|-1/2\rangle - 0.01|-9/2\rangle,$$

$$\mu_{\text{sat}} = 2.36 \mu_B.$$

Now from Fig. 5 the $\Gamma_8^{(2)}$ state is clearly an incorrect assignment. Note that this has the $|9/2\rangle$ state as the major term. For $0.3 < \sin\theta/\lambda < 0.5\text{\AA}^{-1}$ the anisotropy comes primarily from the magnetic quadrupole moment, which is sensed through the $\langle j_2 \rangle$ function. The shape of the magnetization density observed in USb is incompatible with both the $\Gamma_8^{(2)}$ or free-ion $|9/2\rangle$ states. Point-charge calculations give $x > 0$ and $W < 0$ with a $\Gamma_8^{(1)}$ ground state. This is found in all Nd compounds²⁴ (4,3). Our assignment of the ground state is also opposite to that suggested by Troc and Lam²⁵ from an analysis of the high-temperature susceptibility of UP and UAs. However, the present neutron experiments represent the first direct identification of a crystal-field eigenstate in an actinide intermetallic compound.

We have also measured the temperature dependence of Δf . This quantity is very sensitive to the occupation of states with different symmetry from the ground state. In Fig. 6 we show the suggested crystal-field level scheme for USb in the presence of an internal exchange field (the molecular field model). In the absence of H_{exch} the $\Gamma_8^{(1)} - \Gamma_6$ energy separation is ~ 300 K. As H_{exch} is increased the degeneracy of the Γ_8 state is raised, and the gap between the lowest level of the excited Γ_6 state is narrowed. If the Γ_8 state is separated by more than about 500 K from Γ_6 the anisotropy will be temperature independent. On the other hand, in the free-ion picture (which is approached on the extreme right of Fig. 6) the

temperature dependence of the anisotropy is very abrupt, being approximately proportional to the fifth power of the dipole moment at low temperatures. The measured quantity $\Delta f(T)$ is related to the effective quadrupole moment $\langle Q_2 \rangle$ by normalizing, thus $\langle Q_2 \rangle \propto \Delta f(T)/\Delta f(T = 0)$ and this is plotted as a function of the reduced dipole moment in Fig. 7. Note that the experimental $\langle Q_2 \rangle$ shows some temperature dependence, placing an upper limit of ~ 400 K on the $\Gamma_8^{(1)} - \Gamma_6$ energy separation. Using a molecular field model as illustrated in Fig. 6 we have calculated $\Delta f(T)$, and the results for $W = 6, 7$, and 8 K are shown in Fig. 7. Near T_N Δf rapidly diminishes, leading to an increase in the $\Gamma_8^{(1)} - \Gamma_6$ separation, with a corresponding increase in Δf . The data do not reflect this upturn near T_N , but do suggest that $W \sim 7$ K is a reasonable value. The present elastic scattering measurements show the need for single-crystal inelastic neutron experiments because the exchange interactions will undoubtedly produce considerable dispersion in the crystal-field levels. This may well account for the failure to detect crystal-field levels using polycrystalline samples and time-of-flight techniques.²⁶ However, the concept of a well-defined crystal-field state does appear to be valid for antiferromagnetic USb.

As suggested by Table I the Pu ions usually belong to the f^5 configuration. The magnetic cross section for this state is most unusual, having a maximum at $\sin\theta/\lambda \sim 0.3 \text{ \AA}^{-1}$ rather than at zero. The reason is that $L = 5$, $S = 5/2$, and these oppose each other, $J = L - S = 5/2$. The localized magnetization density from the orbital moment is opposed by a large, but diffuse, negative spin density. The total magnetization therefore changes sign as one proceeds away from the nucleus. The Fourier transform of the magnetization density then has a maximum at $K \neq 0$. Since this form factor is unique to the f^5 configuration, neutron scattering provides a simple method of establishing the ground state. Unfortunately, single crystals of Pu compounds have not yet been produced, but in Fig. 8 we show results obtained with polarized neutrons from a polycrystalline sample of ferromagnetic ^{247}PuP . Preferred orientation effects, which establish the easy axis as $\langle 100 \rangle$, limit the number of reflections that can be measured. The smooth curve is a best fit to the data using relativistic $\langle j_i \rangle$ integrals and the $5f^5: ^6H_{5/2}; \Gamma_8$ ground state. This form factor extrapolates to give μ_s at $= 0.62 \mu_B$, the magnetization value²⁷ is $0.42 \mu_B$. In these configurations we will certainly have to take into account the effects of J mixing since estimates²⁸ show that the $^6H_{5/2}$ state may not make up more than $\sim 66\%$ of the ground state. Calculations of the magnetic cross section for these complicated situations are in progress.

SUMMARY

We have concentrated almost exclusively here on the properties of the NaCl actinide compounds. As Table I illustrates, we are able to interpret most of the magnetic properties in terms of localized 5f electrons behavior. However, direct proof of the crystal-field level-picture remains hard to obtain. Even in the so-called simple systems the microscopic exchange and spin-lattice interactions remain totally unresolved. For example, the sudden increase in the ordered magnetic moment in UP at low temperature has been analyzed in terms of both a crystal-field effect²⁸ and a change in the valence state.²⁹ We have discussed the spin-lattice interaction with reference to recent observations¹⁵ on the insulating actinide antiferromagnet UO₂, but the application of these ideas to systems that exhibit effects such as in Fig. 2 will require a substantial theoretical effort. In some cases, e.g., UN, US, and possibly UC and UP, the 5f band is probably broad enough that a simple localized model will not predict the correct magnetic behavior. X-ray photoemission and de Haas van Alphen experiments on these systems should prove most rewarding.

As discussed in the final section, the measurement of the elastic magnetic cross section is providing quantitative information on the radial and angular wave functions of the unpaired 5f electrons. Further experiments of this nature, together with inelastic neutron experiments to measure the elementary excitations, will be most valuable. To accomplish these goals, a much greater effort should be made to grow single crystals.

ACKNOWLEDGMENTS

I am indebted to many colleagues at Argonne National Laboratory for stimulating discussions and collaboration over the years, in particular, A. T. Aldred, M. B. Brodsky, T. O. Brun, B. D. Dunlap, J. Faber, Jr., A. J. Freeman, F. Y. Fradin, D. J. Lam, and M. H. Mueller. The technical assistance of R. L. Hitterman, H. W. Knott, and J. F. Reddy in solving a variety of problems is greatly appreciated.

REFERENCES

*Work performed under the auspices of USERDA.

1. "The Actinides: Electronic Structure and Related Properties," edited by A. J. Freeman and J. B. Darby (Academic Press, New York, 1974), A. J. Freeman and D. D. Koelling, Vol. I, ch. 2.
2. S. K. Chan and D. J. Lam, Ref. 1, Vol. I, ch. 1.
3. H. L. Davis, Ref. 1, Vol. II, ch. 1.
4. D. E. Eastman and M. Kuznietz, Phys. Rev. Letters, 26, 846 (1971), J. Appl. Physics, 42, 1396 (1971).
5. B. Veal, Ref. 1, Vol. II, ch. 3, pp. 101-107.
6. W. J. Nellis and M. B. Brodsky, Ref. 1, Vol. II, ch. 6. M. B. Brodsky, AIP Conf. Proc. 5, 611 (1972).
7. A detailed survey up to 1972 is given by D. J. Lam and A. T. Aldred, Ref. 1, Vol. I, ch. 3. An excellent literature survey of uranium compounds is given by J. Grunzweig-Genossar, M. Kuznietz, and F. Friedman, Phys. Rev. 173, 562 (1968).
8. For the Np compounds see A. T. Aldred, B. D. Dunlap, A. R. Harvey, D. J. Lam, G. H. Lander, and M. H. Mueller, Phys. Rev. B 9, 3766 (1974).
9. For lattice distortions see C. H. Lander and M. H. Mueller, Phys. Rev. B 10, 1994 (1974).
10. H. Hill in "Plutonium 1970 and Other Actinides," edited by W. N. Miner (AlME, New York, 1971) p. 2.
11. B. D. Dunlap and G. H. Lander, Phys. Rev. Letters, 33, 1046 (1974).
12. A. T. Aldred, B. D. Dunlap, D. J. Lam, G. H. Lander, M. H. Mueller and I. Nowik, Phys. Rev. B 11, 530 (1975).
13. See, for example, B. R. Cooper and O. Vogt, Phys. Rev. B 1, 1218 (1970).
14. J. A. Marples, C. F. Sampson, F. A. Wedgwood, and M. Kuznietz, J. Phys. C 8, 708 (1975).
15. J. Faber, Jr., G. H. Lander, and B. R. Cooper, see paper in this Conference.
16. S. J. Allen, Phys. Rev. 166, 530 (1968); 167, 492 (1968); R. A. Cowley and G. Dolling, Phys. Rev. 167, 464 (1968).
17. K. W. H. Stevens and E. Pytte, Solid State Comm. 13, 101 (1973).
18. W. Marshall and S. W. Lovesey, "Theory of Thermal Neutron Scattering," (Oxford U.P., London, 1971); G. H. Lander, T. O. Brun and O. Vogt, Phys. Rev. B 7, 1988 (1973) and references therein.
19. A. J. Freeman, J. P. Desclaux, G. H. Lander, and J. Faber, Jr., Phys. Rev. B (in press).
20. O. Steinvoil, G. Shirane, R. Nathans, M. Blume, H. A. Alperin, and S. J. Pickart, Phys. Rev. 161, 499 (1967)

21. E. Balcar, J. Phys. C 8, 1581 (1975).
22. G. H. Lander, J. Faber, Jr., A. J. Freeman and J. P. Desclaux, Phys. Rev. B (in press).
23. F. A. Wedgwood, J. Phys. C 5, 2427 (1972).
24. A. Furrer, J. Kjems, and O. Vogt, J. Phys. C 5, 2246 (1972); J. Phys. C 7, 3365 (1974); J. Phys. C 8, 1054 (1975).
25. R. Troc and D. J. Lam, Phys. Stat. Solidi B 65, 317 (1974).
26. F. A. Wedgwood, J. Phys. C 7, 3203 (1974).
27. D. J. Lam, F. Y. Fradin, and O. L. Kruger, Phys. Rev. 187, 606 (1969).
28. C. Long and Y. L. Wang, Phys. Rev. B 3, 1656 (1971).
29. J. M. Robinson and P. Erdos, Phys. Rev. B 8, 4333 (1973); Phys. Rev. B 9, 2187 (1974).

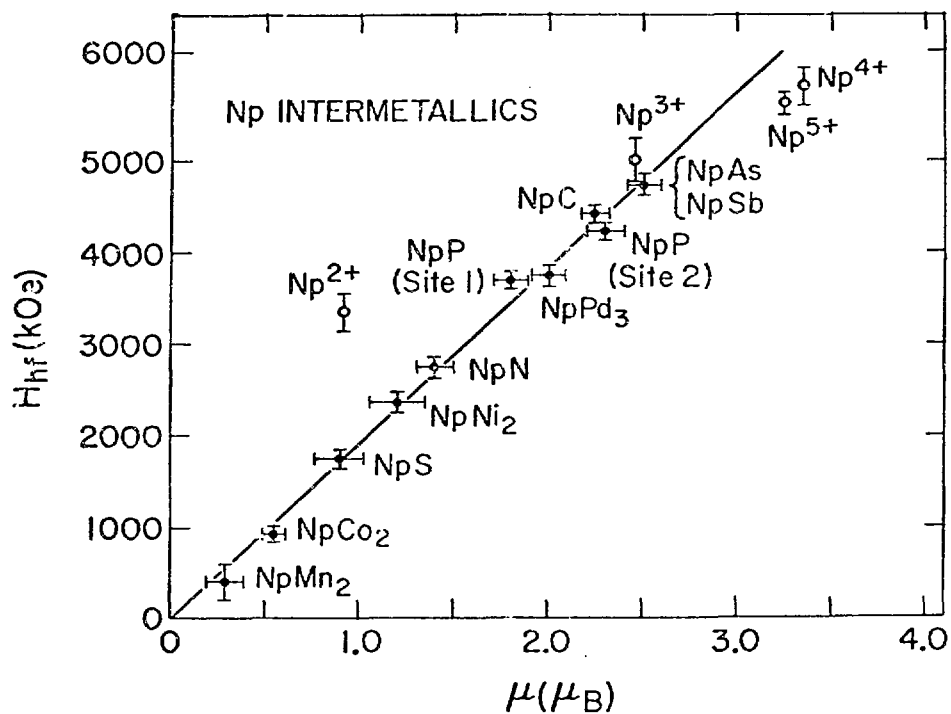


Fig. 1. Linear relationship between the hyperfine field H_{hf} and the magnetic moment μ in neptunium intermetallics. Experimental points are shown by closed circles and calculated free-ion values by open circles.

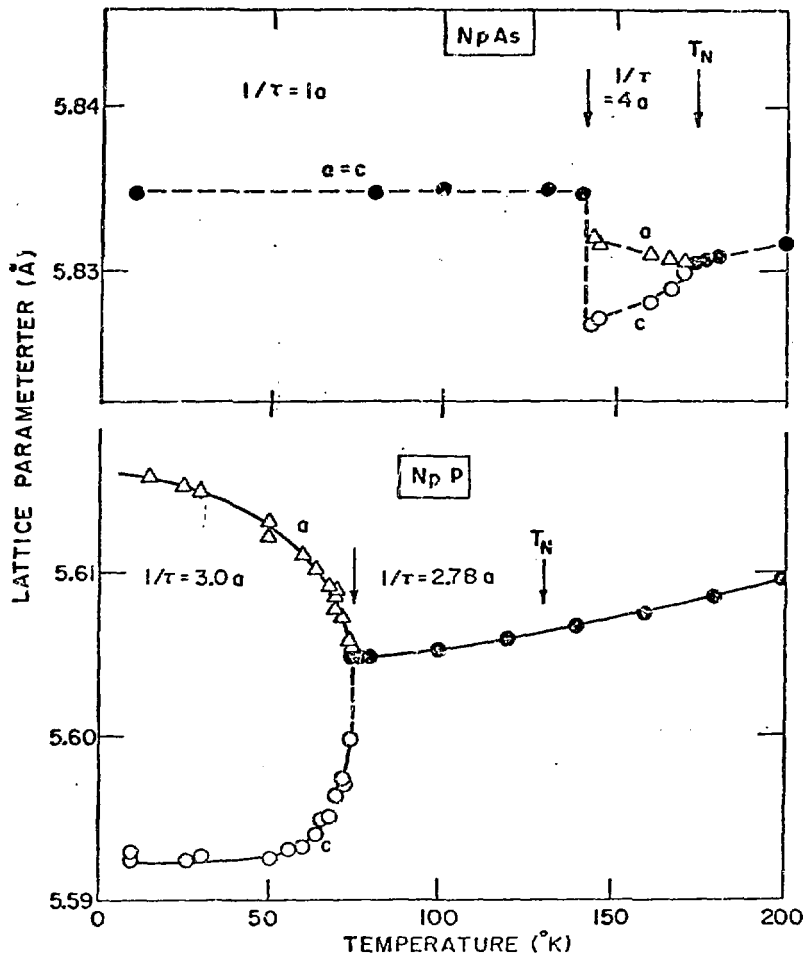


Fig. 2. Lattice parameters of NpP and NpAs as a function of temperature. The quantity $1/\tau$ gives the repeat distance of the magnetic structure.

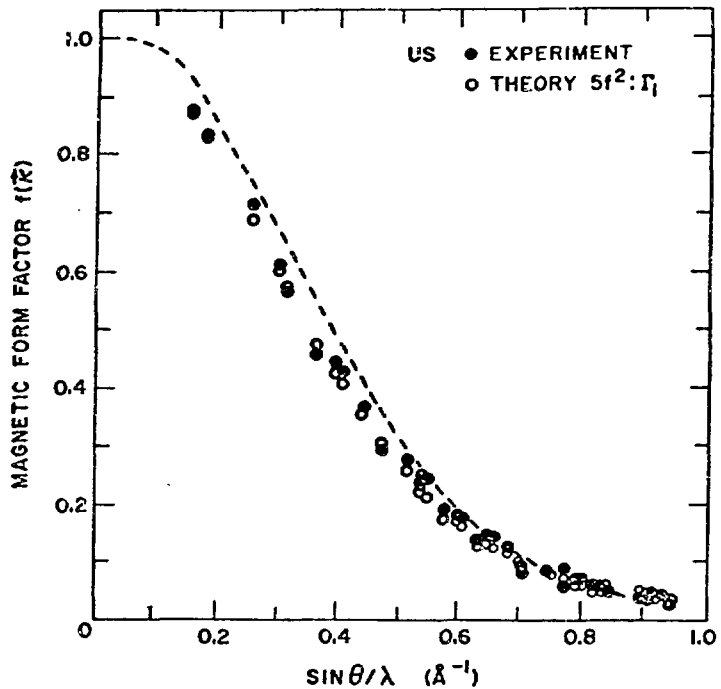


Fig. 3. Magnetic form factor for US. The solid points are from Wedgwood (Ref. 23) using a magnetic moment of $1.70 \mu_B$. The open points are obtained with a $5f^2:3H_4:5I_1$ plus exchange model and the relativistic $\langle j_i \rangle$ functions of Ref. 19. The broken line is a smooth curve drawn through the theoretical form factor of the $5f^4:5I_4$ configuration.

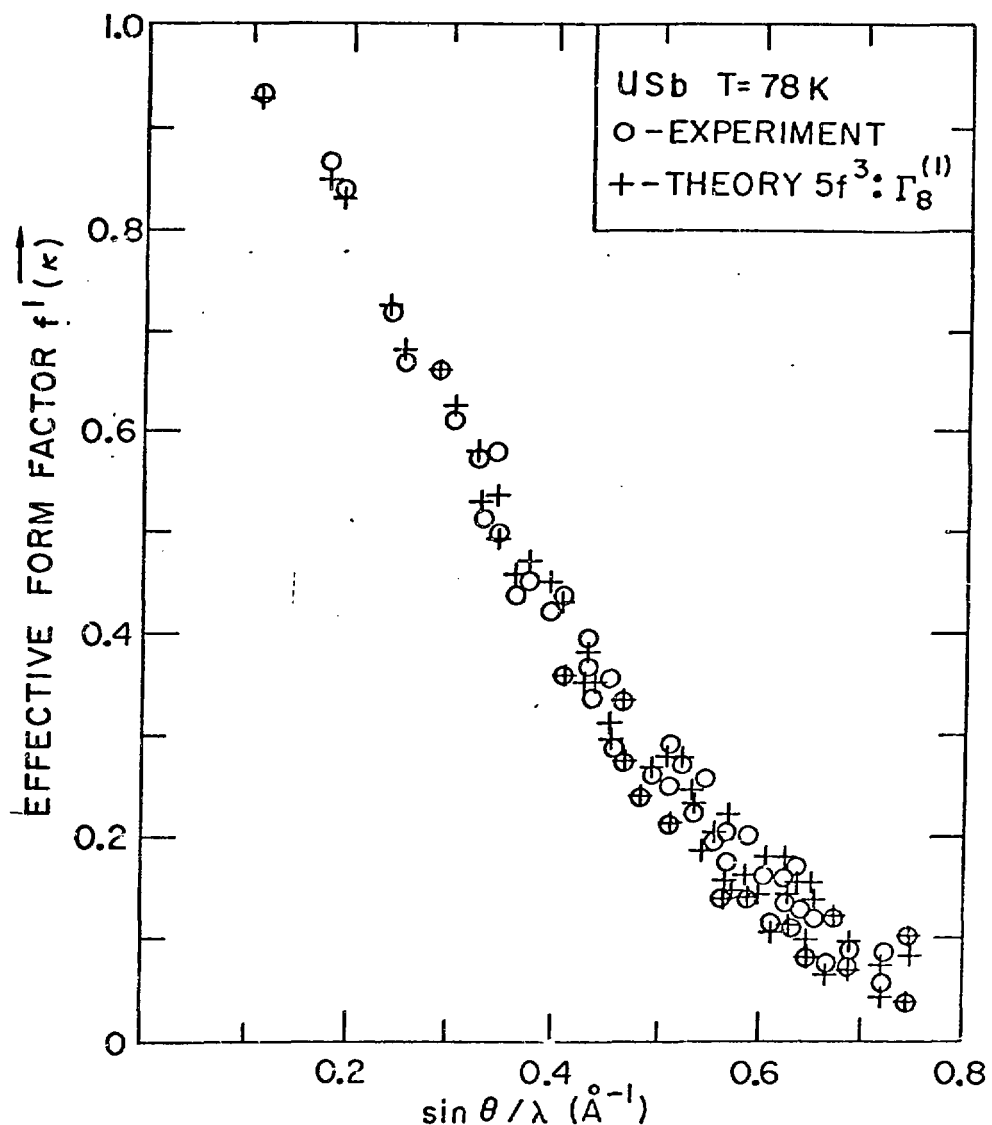


Fig. 4. Effective magnetic form factor of USb. The relativistic integrals of Ref. 19 have been used together with the $5f^3: \Gamma_8^{(1)}$ configuration.

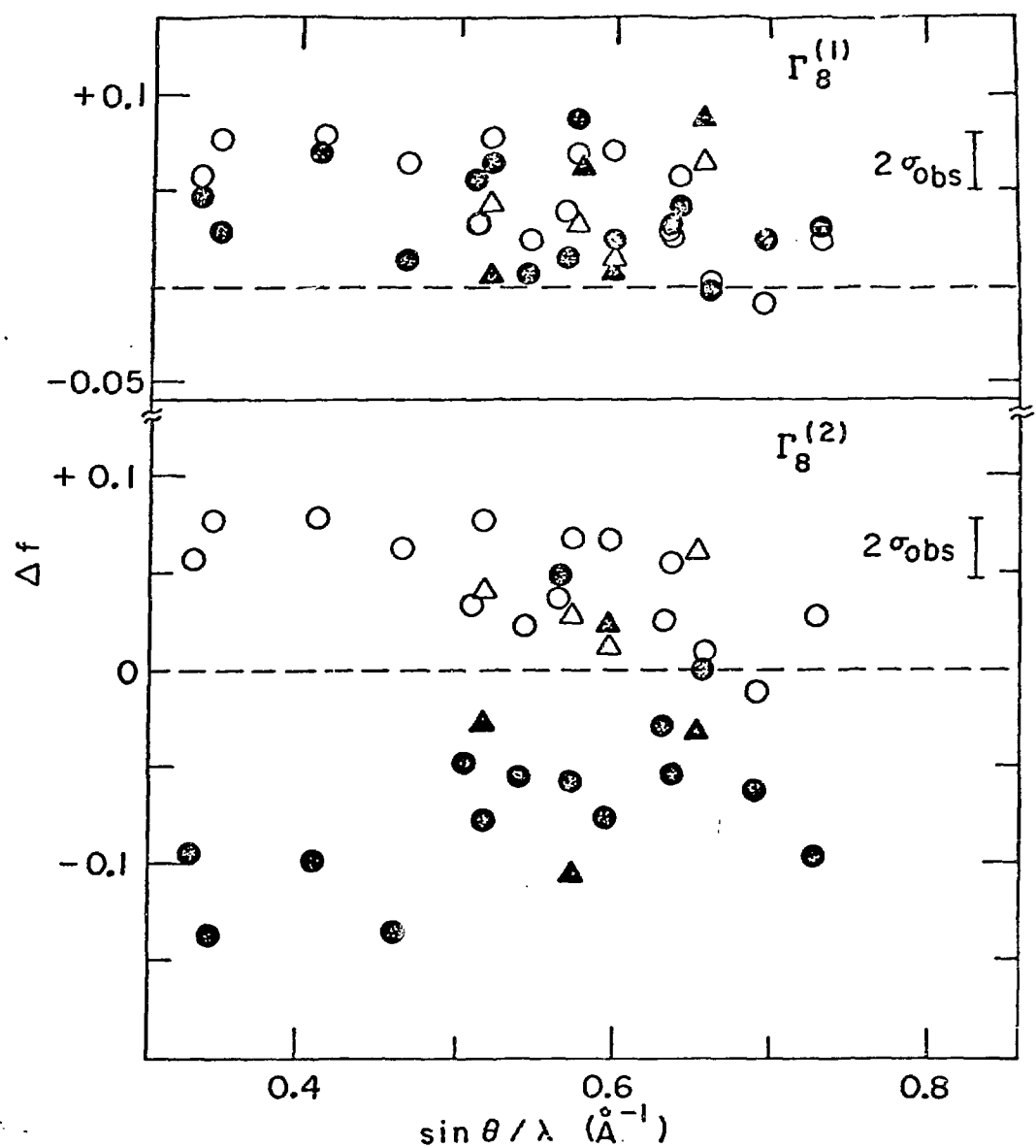


Fig. 5. Anisotropy in the form factor of USb. Δf is defined in Eq. (5). The open points are the experimental values, the solid points those calculated with the $\Gamma_8^{(1)}$ (upper plot) and $\Gamma_8^{(2)}$ (lower plot) ground state eigenfunctions.

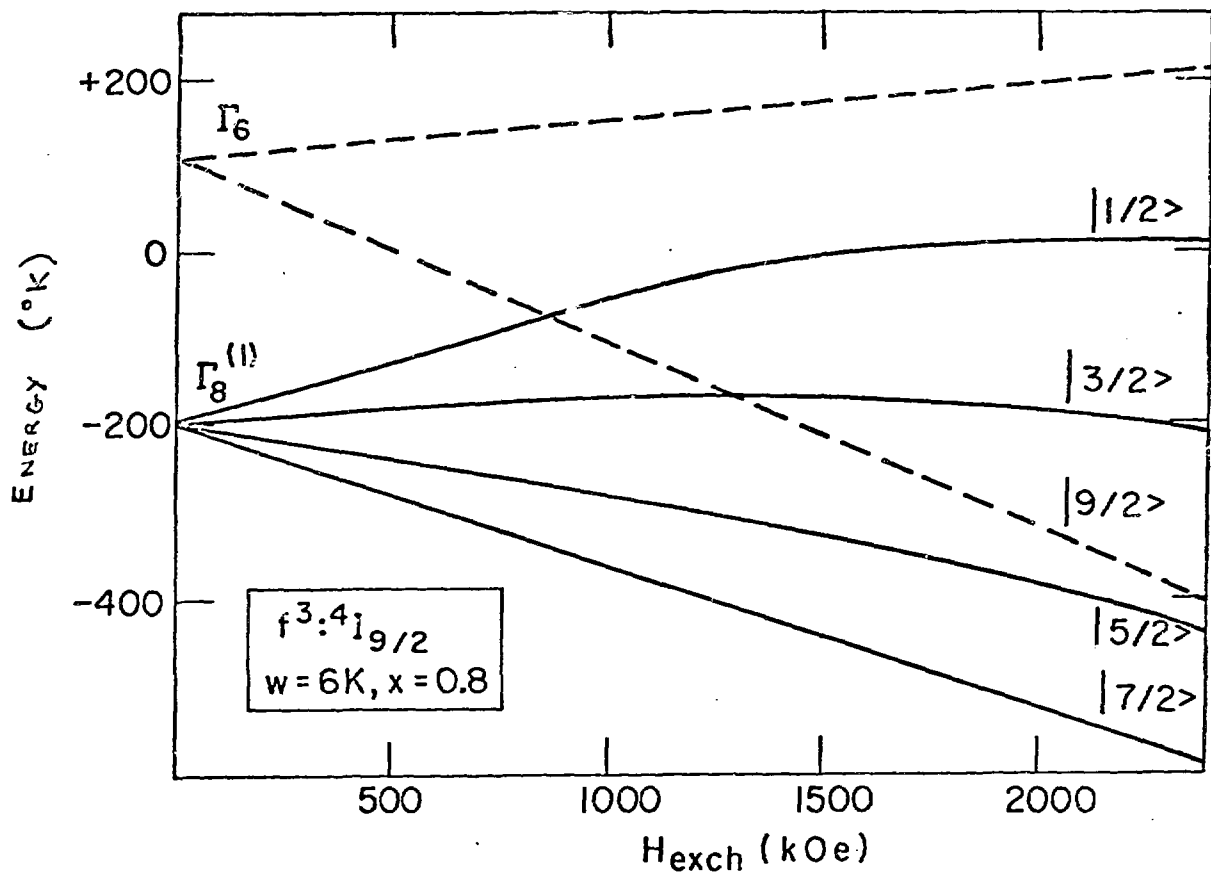


Fig. 6. Variation of the crystal-field levels with an internal exchange field. The $\Gamma - \Gamma^{(1)}$ splitting at $H = 0$ represents that proposed for USb. As $H_{\text{exch}} \rightarrow \infty$ the eigenfunctions have the character indicated on the right-hand-side of the diagram. (The higher $\Gamma^{(2)}$ crystal-field level is not shown.)

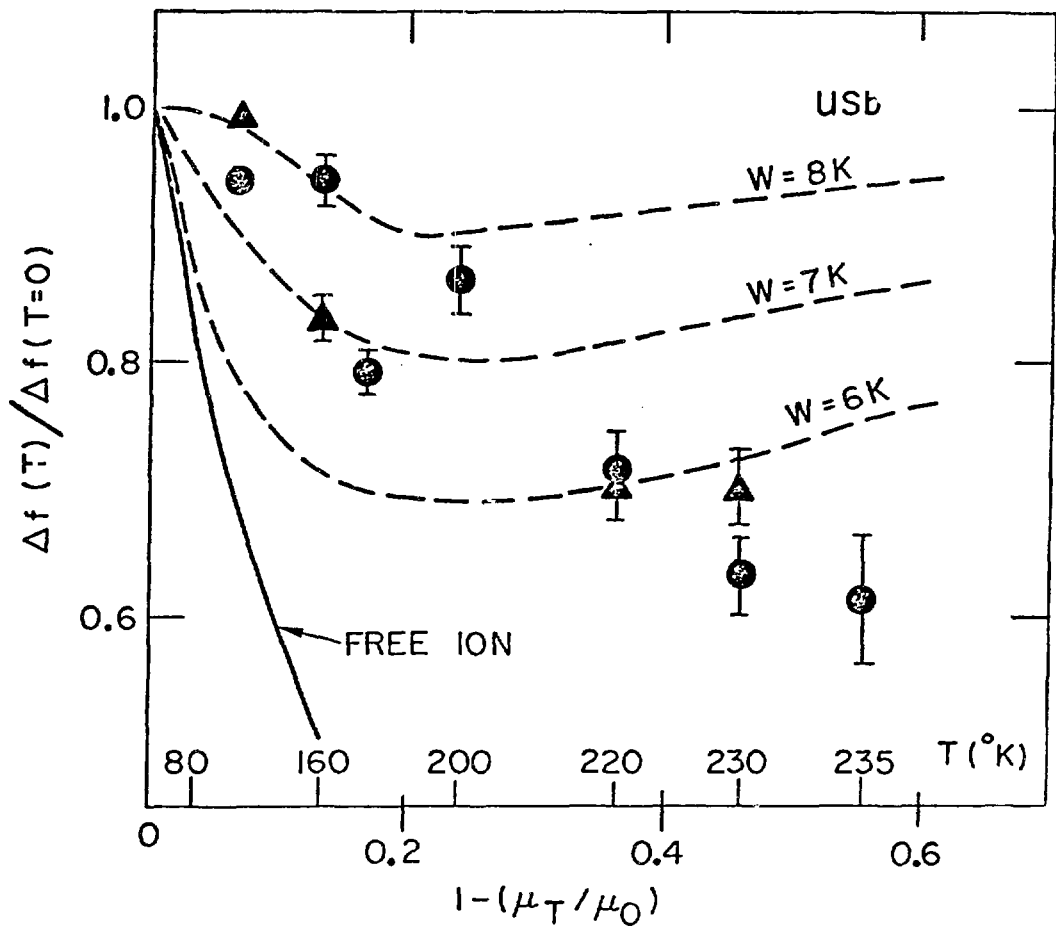


Fig. 7. Variation of the form factor anisotropy as a function of the dipole moment (temperature is an implicit parameter). The circles and triangles represent different pairs of Bragg reflections. The solid line is the free-ion result, the broken curves calculations using the crystal-field levels of Fig. 6 and a simple molecular-field model.

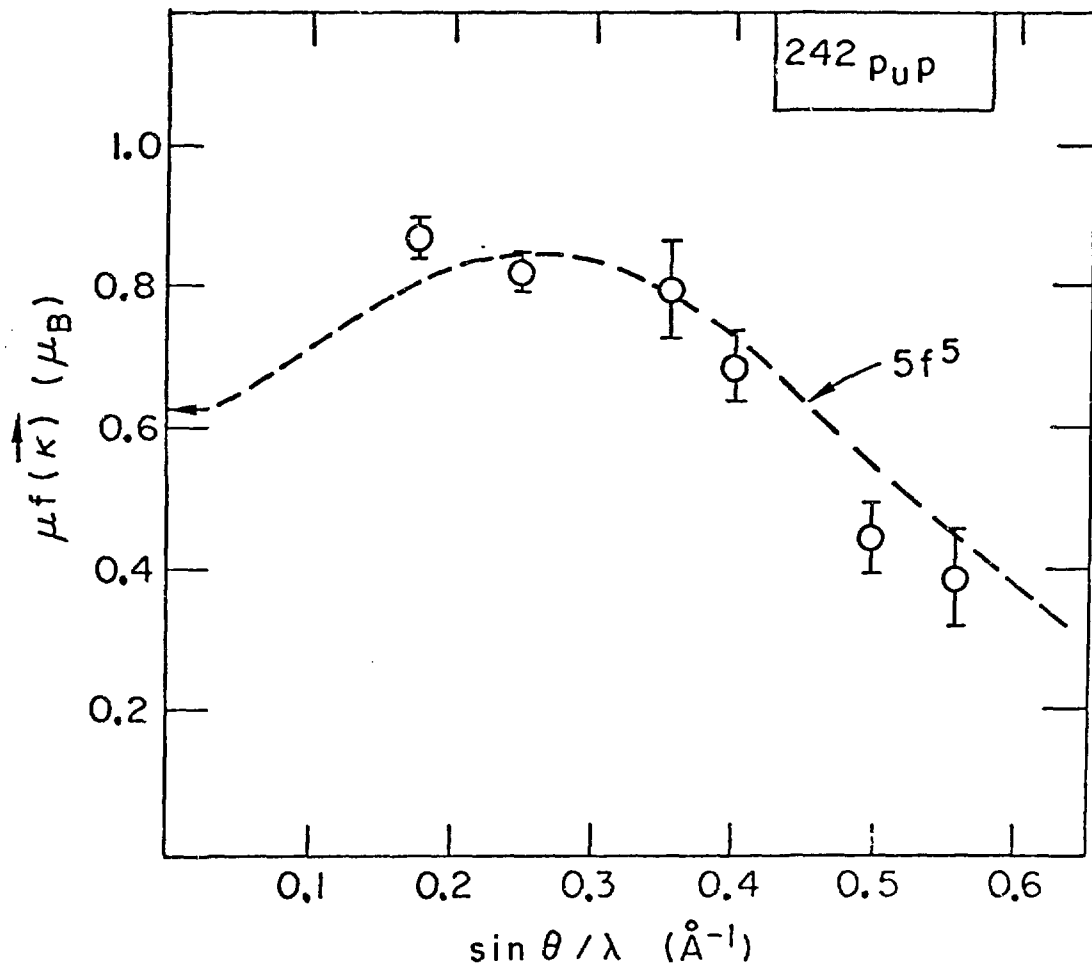


Fig. 8. Results of polarized neutron experiment on ^{242}PuP .

Table I. Magnetic properties of NaCl actinide compounds. For a rhombohedral distortion, easy axis $\langle 111 \rangle$, c and a are defined here as distances measured parallel and perpendicular to the trigonal axis such that $c/a = 1$ in the cubic phase.

	$\frac{a}{c}$ (\AA)	Magnetism	Temp. ($^{\circ}\text{K}$)	μ_{eff} (μ_{B})	μ_{sat} (μ_{B})	Easy Axis	$1-c/a$ ($\times 10^4$)	f^{r}
UC	4.960	TIP	---	---	---	---	---	2
UN	4.890	AF I	53	3.1	0.75	$\langle 100 \rangle$	-6	2?
UP	5.589	AF I	125	2.2	1.9	$\langle 100 \rangle$	<5	3
UAs	5.779	AF I IA	127 63	3.4	1.9 2.2	$\langle 100 \rangle$	<5	3
USb	6.197	AF I	241	~ 3.8	2.8	$\langle 100 \rangle$?	3
US	5.489	F	178	2.25	1.70	$\langle 111 \rangle$	+105	2?
USE	5.744	F	160	~ 2.4	2.0	$\langle 111 \rangle$	+81	3?
NpC	5.000	AF I F	310 220	3.4	2.1	$\langle 100 \rangle$ $\langle 111 \rangle$	<5 +23	4?
NpN	4.897	F	87	2.4	1.4	$\langle 111 \rangle$	-52	4?
NpP	5.615	AF 3+3-	130	2.8	1.8 2.3	$\langle 100 \rangle$	-42	4
NpAs	5.838	AF 4+4- I	175 142	~ 2.6	2.5	$\langle 100 \rangle$ $\langle 100 \rangle$	-8 ≤ 3	4
NpSb	6.254	AF I	207	~ 2.3	2.5	$\langle 100 \rangle$	<15	4
NpS	5.527	AF II	20	2.2	0.9	$\langle 100 \rangle$	<5	4?
PuC	4.977	AF I	~ 100	~ 1	0.8	$\langle 100 \rangle$?	5
PuN	4.905	AF ?	13	1.1	?	?	?	5
PuP	5.659	F	126	1.1	~ 0.5	$\langle 100 \rangle$?	5
PuSb	6.240	F	85	1.0	0.6	?	?	5
PuS	5.537	TIP	---	---	---	---	---	6
AmSb	6.239	TIP	---	---	---	---	---	6

TIP--temperature independent paramagnetism.

AF --antiferromagnetism, I - type I + -; IA - type IA 2+ 2-; II - type II; F - ferromagnetism.